Survey of strong normal-internal $k : \ell$ resonances in quasi-periodically driven oscillators for $\ell = 1, 2, 3$.

H.W. BROER* and R. VAN DIJK

Institute for mathematics and computing sciences, University of Groningen, The Netherlands
**E-mail: broer@math.rug.nl*
http://www.math.rug.nl/~broer

R. VITOLO

Dipartimento di Matematica e Informatica, Università di Camerino, Italy
E-mail: renato.vitolo@unicam.it

Recently, semi-global results have been reported by Wagener[6] for the $k : \ell$ resonance where $\ell = 1, 2$. In this work we add the $\ell = 3$ strong resonance case and give an overview for $\ell = 1, 2, 3$. For an introduction to the topic, as well as results on the non-resonant and weakly-resonant cases, see Refs. 1,2,6.

Keywords: Quasi-periodically driven oscillators; *Duffing - Van der Pol* oscillator; 'Stoker's response problem'; strong resonance.

1. Introduction to the problem

We consider the forced *Duffing - Van der Pol* oscillator, given by

$$\begin{cases} \dot{x}_j = \omega_j, \qquad j = 1, \ldots, m, \\ \dot{y}_1 = y_2, \\ \dot{y}_2 = -(a + cy_1^2)y_2 - by_1 - dy_1^3 + \varepsilon f(x_1, \ldots, x_m, y_1, y_2, a, b, c, d, \varepsilon), \end{cases} \tag{1}$$

which is a vector field defined on $\mathbb{T}^m \times \mathbb{R}^2 = \{(x_1, \ldots, x_m), (y_1, y_2)\}$. Here f is a smooth function which is 2π-periodic in its first m-arguments. We take $\sigma = (a, b)$ as parameter, ε as perturbation parameter and (c, d) as coefficients. The internal frequency vector $\omega = (\omega_1, \ldots, \omega_m)$ is to be non-resonant, or quasi-periodic. The search is for quasi-periodic response solutions, i.e. invariant m-tori of (1), with frequency vector ω, that can be represented as graphs $y = y(x)$ over $\mathcal{T} = \mathbb{T}^m \times \{0\}$. For large values of $|a|$ we can use a contraction argument. However, if $|a| \ll 1$ this approach fails due to small divisors. Braaksma and Broer[1] use KAM theory to find invariant tori for small $|a|$. This requires *Diophantine* non-resonance conditions on the frequency vector ω and the normal frequencies. The case $a \approx 0$ involves a Hopf bifurcation of the corresponding free oscillator ($\varepsilon = 0$). We generalise the above setup by considering the family of vector fields

$$X_{\sigma,\epsilon}(x,y) = \omega\partial_x + (A(\sigma)y + B(y,c,d) + \varepsilon F(x,y,\sigma,c,d,\varepsilon))\partial_y, \qquad (2)$$

where again $(x,y) \in \mathbb{T}^m \times \mathbb{R}^2$, and σ, ε, (c,d) are taken as before. The normal linear part of the unperturbed invariant torus $\mathcal{T}$ is given by

$$N_\sigma(x,y) = \omega\partial_x + A(\sigma)y\partial_y.$$

Let $\lambda = \mu(\sigma) \pm i\alpha(\sigma)$ denote the eigenvalues of $A(\sigma)$ where $\alpha(\sigma)$ is called the normal frequency. We assume that the map $\sigma \mapsto (\mu(\sigma), \alpha(\sigma))$ is a submersion, which allows to take (μ, α) as parameters instead of σ. A normal-internal $k : \ell$ resonance of $\mathcal{T}$ occurs if

$$\langle k, \omega\rangle + \ell\alpha(\sigma) = 0 \qquad (3)$$

for $k \in \mathbb{Z}^m \setminus \{0\}$ and $\ell \in \mathbb{Z}\setminus\{0\}$. The smallest integer $|\ell|$ for which (3) holds, is called the order of the resonance. Resonances up to order 4 are called strong. The non-resonant and weakly resonant cases have been investigated in Ref. 1. Here we consider resonances such that (3) holds for $|\ell| = 1, 2$ and 3. Therefore we assume that at $\sigma = \sigma_0$ the normal part N_{σ_0} of X versally unfolds a Hopf bifurcation at $y = 0$ and that torus $\mathcal{T}$ is at strong normal-internal resonance.

To study (2), an averaging procedure is followed to push time dependence to higher order terms. Next a *Van der Pol* transformation is applied to bring the normal frequencies close to zero. Using a suitable complex variable z, the vector field X transforms to

$$X_{\lambda,\theta,\delta}(x,z) = \omega\partial_x + \delta^2\Re(\lambda z + e^{i\theta_0}|z|^2 z + \bar{z}^{\ell-1})\partial_z + \delta^3\tilde{Z}(x,z).$$

For details see Wagener.[6] Here θ_0 is a generic constant, $\lambda = \mu + i\alpha$ a parameter and $\delta = \varepsilon^{\ell-4}$ is a rescaled perturbation parameter. All non-integrable terms are truncated, yielding the so-called 'principal part':

$$Z_0 = \Re(\lambda z + e^{i\theta_0}|z|^2 z + \bar{z}^{\ell-1})\partial_z. \qquad (4)$$

In the next section we describe the bifurcation diagrams of Z_0 for $\ell = 1, 2$ and 3 summarising results from Refs. 2,3,6, for a periodic analogue see Gambaudo.[5] Bifurcations of equilibria of Z_0 correspond to bifurcations of quasi-periodic m-tori of the integrable vector field $\omega\partial_x + Z_0$. This interpretation remains valid if we add integrable perturbations. However, adding non-integrable (δ^3) terms breaks the torus symmetry and quasi-periodic bifurcation theory has to be invoked. For persistence results see Ref. 2.

Table 1. Notation used for the codimension one bifurcation curves (leftmost two columns) and codimension two points (rightmost two columns) for all figures in Sec. 2.

Notation	Name	Notation	Name
HE_1	Heteroclinic	BT_2	Bogdanov-Takens
L_1	Homoclinic bifurcation	DL_2	Degenerate homoclinic
H_1	Hopf bifurcation	H_2	Degenerate Hopf
PF_1	Pitchfork	PF_2	Degenerate Pitchfork
SN_1	Saddle Node (Fold)	SN_2	Cusp
$SNLC_1$	Saddle node of limit cycles	L_2	Homoclinic at saddle node
		SDZ_2	Symmetric double zero

2. Results

In the previous section a normal form truncation (4) was introduced for the general family of vector fields (2) at normal-internal resonance. Here we present the bifurcation diagram of (4) in the (μ, α)-plane (we recall that $\lambda = \mu + i\alpha$) for $\ell = 1, 2, 3$. However, in certain cases the coefficient θ_0 is sometimes 'activated' as an extra parameter. For the $k : 1$ resonance, this gives rise to a codimension three bifurcation point of nilpotent elliptic type, which can be seen as an 'organising centre'. Auxiliary variables ζ, $\psi \in \mathbb{R}$ and $\rho \in \mathbb{C}$ are introduced by setting

$$\zeta = |z|^2, \quad z = \sqrt{\zeta} e^{i\psi}, \quad \rho = \rho_1 + i\rho_2 = e^{-i\theta_0}\lambda,$$

see Refs. 2,6. The bifurcation diagrams are reported at the end of the paper and the notation used there is summarized in Table 1. Local bifurcations are obtained analytically, while global bifurcations are found and continuated by standard numerical tools such as AUTO.[4] Proofs of the cases $\ell = 1, 2$ are given in Ref. 2, whereas the case $\ell = 3$ is treated in Refs. 3,5.

2.1. *The k : 1 resonance*

For $\ell = 1$ the family (4) rewrites to

$$\dot{z} = \lambda z + e^{i\theta_0}|z|^2 z + 1. \tag{5}$$

System (5) is symmetric with respect to the group generated by

$$(t, z, \lambda, \theta_0) \mapsto (t, \bar{z}, \bar{\lambda}, -\theta_0) \quad \text{and} \quad (t, z, \lambda, \theta_0) \mapsto (-t, -z, -\lambda, \theta_0 + \pi).$$

Hence, we can restrict θ_0 to $0 \le \theta_0 \le \frac{\pi}{2}$. Two types of local codimension one bifurcations occur in system (5):

(1) a saddle node bifurcation SN_1, given by

$$\rho_1^4\rho_2^2 + 2\rho_1^2\rho_2^4 + \rho_2^6 + \rho_1^3 + 9\rho_1\rho_2^2 + \tfrac{27}{4} = 0;$$

(2) a Hopf bifurcation (with two branches H_1^a and H_1^b), given by

$$\mu^3 - 4\mu^2\alpha\cos\theta_0\sin\theta_0 + 4\mu\alpha^2\cos^2\theta_0 + 8\cos^3\theta_0 = 0,$$
$$2(\alpha - \mu\tan\theta_0)^2 - (\mu\sec\theta_0)^2 > 0.$$

Three types of local codimension two bifurcations occur for (5):

(1) two cusp points SN_2^+ and SN_2^-, depending on θ_0, given by

$$SN_2^\pm: \ \mu = -\tfrac{3}{2}\cos\theta_0 \pm \tfrac{\sqrt{3}}{2}\sin\theta_0, \quad \alpha = -\tfrac{3}{2}\sin\theta_0 \mp \tfrac{\sqrt{3}}{2}\cos\theta_0;$$

(2) two Bogdanov-Takens points BT_2^+ and BT_2^-, given by

$$BT_2^\pm: \ \mu = -\frac{2\cos\theta_0}{(2 \pm 2\sin\theta_0)^{\frac{1}{3}}}, \quad \alpha = -\frac{2\sin\theta_0 + 1}{(2 \pm 2\sin\theta_0)^{\frac{1}{3}}};$$

(3) a degenerate Hopf-bifurcation point H_2 given by

$$H_2: \ \mu = -2\cos\theta_0, \quad \alpha = 0, \quad \tfrac{\pi}{6} < \theta_0 < \tfrac{\pi}{2}.$$

In the restricted parameter space (μ, α, θ_0) there exists a unique codimension three singularity of nilpotent elliptic type. In Fig. 1 the bifurcation diagram is presented along with the codimension two bifurcation points.

2.2. *The $k : 2$ resonance*

For $\ell = 2$ the family (4) rewrites to

$$\dot{z} = \lambda z + e^{i\theta_0}|z|^2 z + \bar{z}. \tag{6}$$

System (6) is symmetric with respect to the group generated by

$$(z, \lambda, \theta) \mapsto (\bar{z}, \bar{\lambda}, -\theta) \quad \text{and} \quad (z, \lambda, \theta) \mapsto (-z, \lambda, \theta).$$

Hence, we can restrict θ_0 to $0 \le \theta_0 \le \pi$. We have depicted the bifurcation diagram in Fig. 3. Three types of local codimension one bifurcations occur in system (6):

(1) a curve of pitchfork bifurcations PF_1, given by $|\rho| = 1$;
(2) two curves of saddle-node bifurcations SN_1, given by $\rho_2^2 = 1, \ \rho_1 < 0$;
(3) three Hopf bifurcation curves H_1, two are given by $\Re(e^{i\theta_0}\rho) = 0$, $|\rho| > 1$, and the third by

$$\tfrac{1}{4}(\rho_1 + \rho_2\tan\theta_0)^2 + \rho_2^2 = 1,$$
$$\tfrac{1}{2}\rho_1^2 + \tfrac{1}{2}\tan\theta_0\rho_1\rho_2^2 < 1, \quad \rho_2\tan\theta_0 - \rho_1 > 0.$$

Moreover, the following codimension two bifurcations take place:

(1) Two degenerate pitchfork bifurcation points PF_2 at $\rho = \pm i$.
(2) Two symmetric double-zero bifurcation points SDZ_2 at $\lambda = \pm i$.
(3) A Bogdanov-Takens bifurcation point BT_2 at $\rho = |\tan\theta_0|(1 + i\cot\theta_0)$.

2.3. *The k : 3 resonance*

For $\ell = 3$ the family (4) rewrites to

$$\dot{z} = \lambda z + e^{i\theta_0}|z|^2 z + \bar{z}^2. \tag{7}$$

System (7) is symmetric with respect to the group generated by

$$(t, z, \lambda, \theta) \mapsto (t, \bar{z}, \bar{\lambda}, -\theta) \text{ and } (t, z, \lambda, \theta) \mapsto (-t, -z, -\lambda, -\theta + \pi).$$

Hence, we can restrict θ_0 to $0 \le \theta_0 \le \frac{\pi}{2}$. Two types of local codimension one bifurcations, depending on θ_0, occur in system (7):

(1) a saddle-node bifurcation curve SN_1, given by $\rho_1 = -\rho_2^2 + \frac{1}{4}$;
(2) a Hopf curve H_1, given by $\Re(\rho e^{i\theta_0} + 2\zeta e^{i\theta_0}) = 0$, $\zeta + \rho_1 - \frac{1}{2} > 0$.

If $\theta_0 \le \frac{\pi}{3}$ there is no Hopf bifurcation of a non-central equilibrium, while the central equilibrium always undergoes Hopf bifurcation for $\mu = 0$. Furthermore, there are two Bogdanov-Takens points BT_2 given by

$$BT_2^{\pm}: \ \rho_2 = \tfrac{1}{2}(\tan\theta_0 \pm \sqrt{\tan^2\theta_0 - 3}).$$

We consider two scenarios: the first corresponds to $\theta_0 \le \frac{\pi}{3}$. Here, the non-central equilibria will not have Hopf bifurcations and, as a result, no Bogdanov-Takens bifurcations occur, see Fig. 4. The second scenario, depicted in Fig. 5, corresponds to $\theta_0 > \frac{\pi}{3}$. Here there are Hopf as well as Bogdanov-Takens bifurcations and the latter involve the occurrence of additional phenomena of global nature. See Ref. 3 for proofs and details.

References

1. B.L.J. Braaksma and H.W. Broer, *Ann. Inst. Henri Poincaré, Analyse non linéare* **4(2)** (1987), 114-168.
2. H.W. Broer, V. Naudot, R. Roussarie, K. Saleh and F.O.O. Wagener, *IJAMAS* (2007), to appear.
3. R. van Dijk, *master thesis*, Universiteit Groningen, (2007).
4. E.J. Doedel et al., *AUTO2000*, `http//indy.cs.concordia.ca`.
5. J.M. Gambaudo, *J. Diff. Eqn.* **57** (1985), 172-199.
6. F.O.O. Wagener, *Global Analysis of Dynamical Systems, Festschrift dedicated to Floris Takens for his 60th birthday*, Bristol and Philadelphia IOP (2001), 167-210.

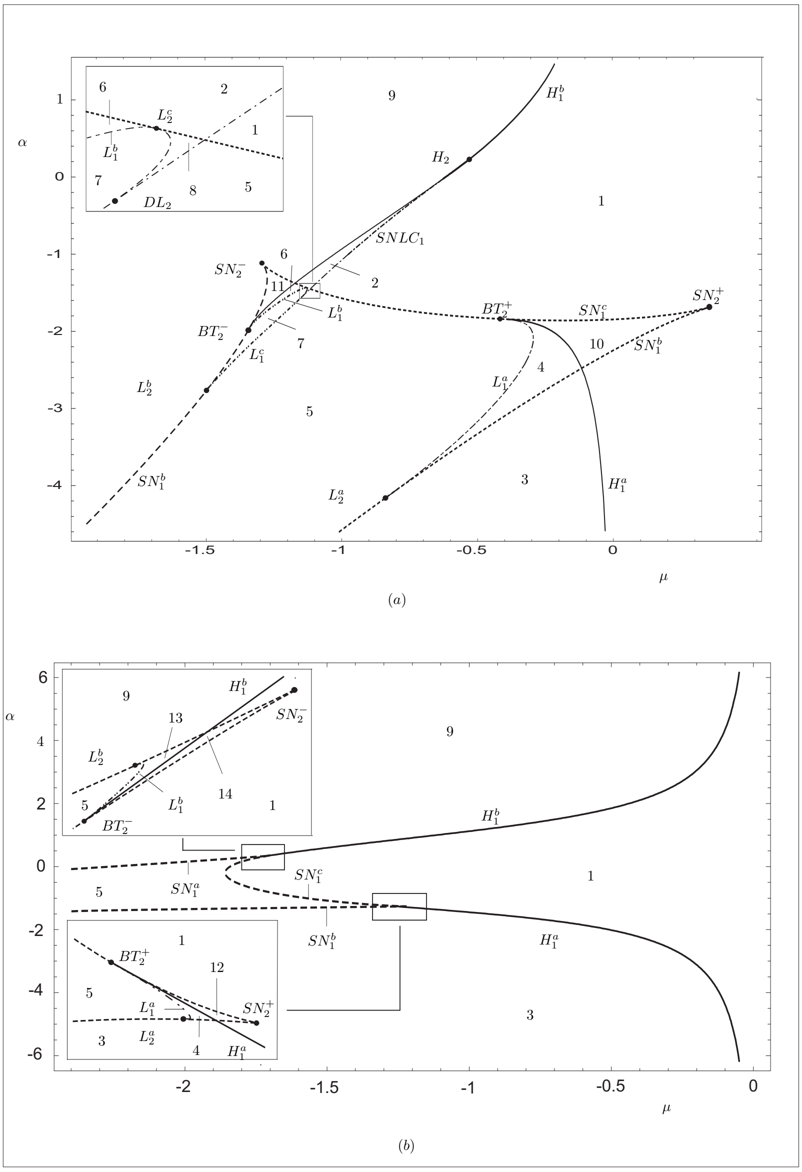

Fig. 1. Two-dimensional bifurcation diagram of the 'principal part' (4) for the k : 1 resonance (5) for two values of θ_0; $(a) : \theta_0 = 2\pi/5$ and $(b) : \theta_0 = \pi/10$. Phase portraits for the noted regions are given in Fig. 2, for the notation we refer to Table 1.

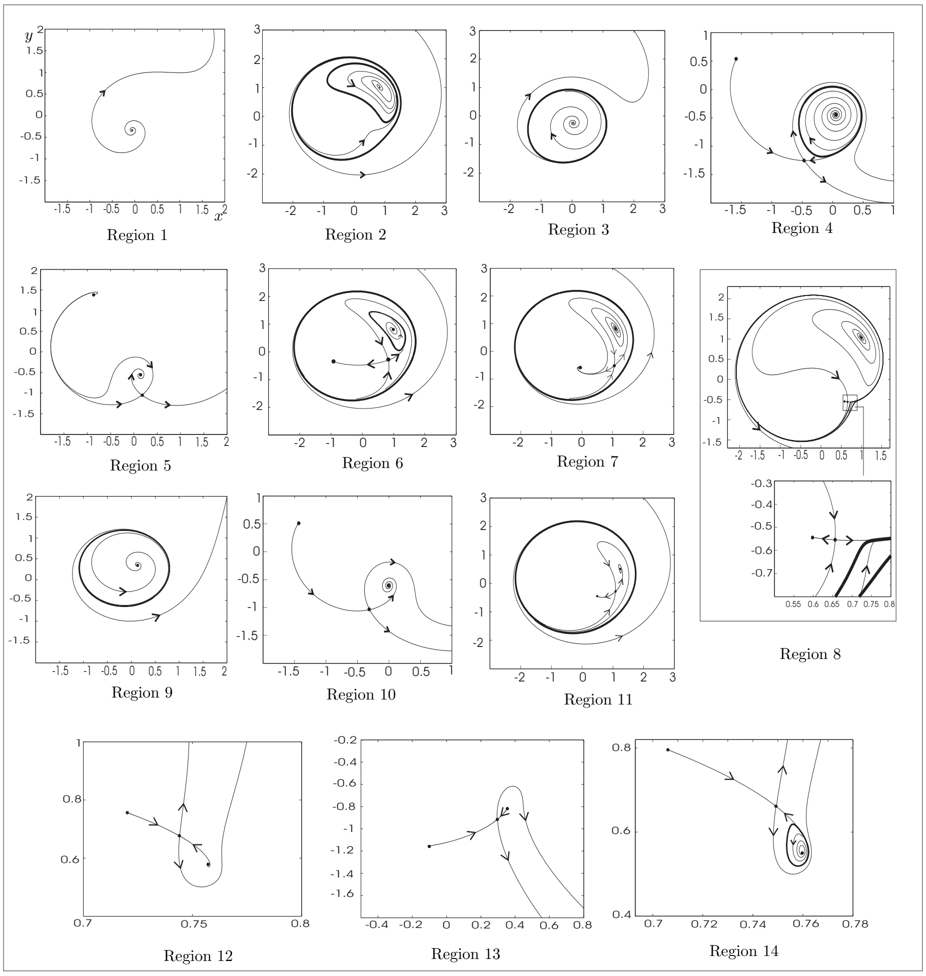

Fig. 2. Phase portraits of the 'principal part' for the $k : 1$ resonance (5). The labels "Region 1 … 14" correspond to the regions in the bifurcation diagram in Fig. 1.

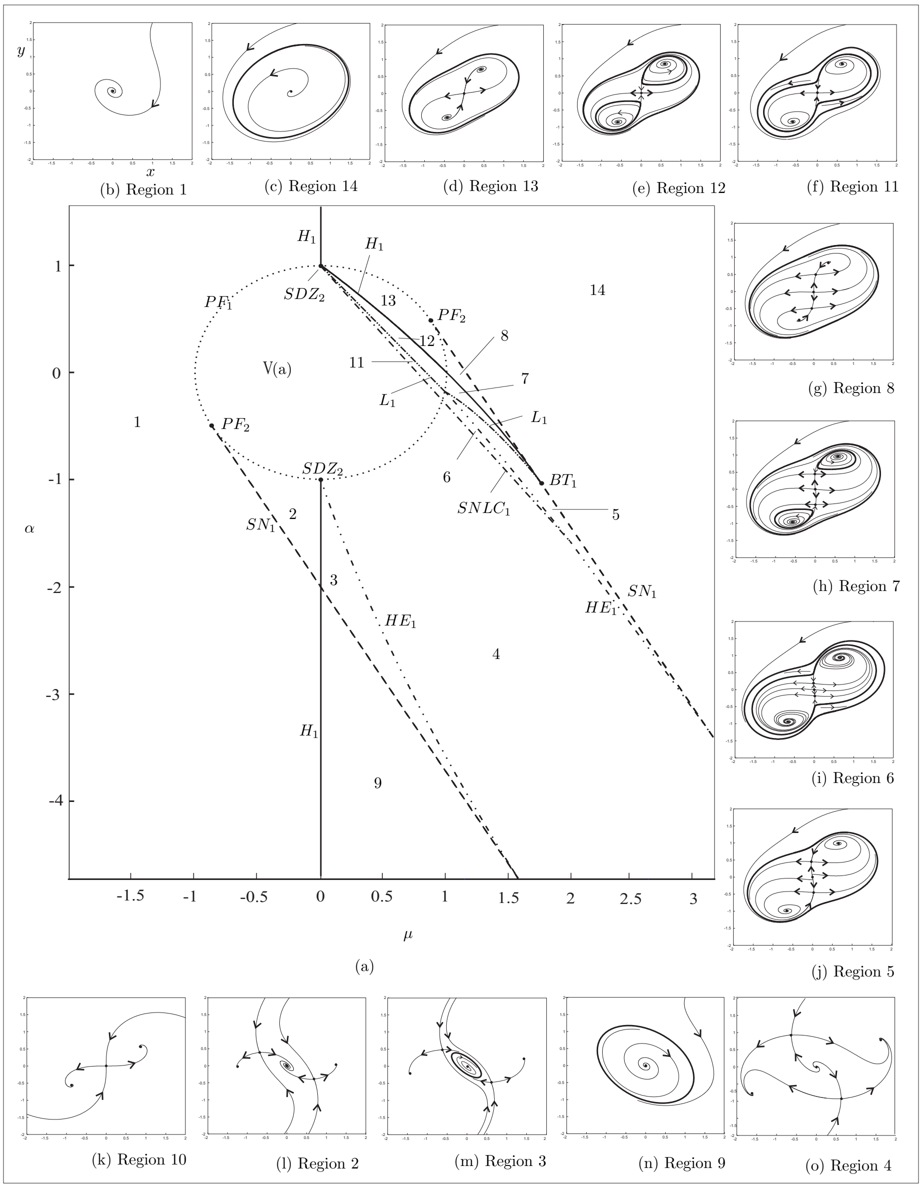

Fig. 3. (a) Two-dimensional bifurcation diagram of the 'principal part' for the $k : 2$ resonance (6); (b)-(o) Phase portraits for the indicated regions.

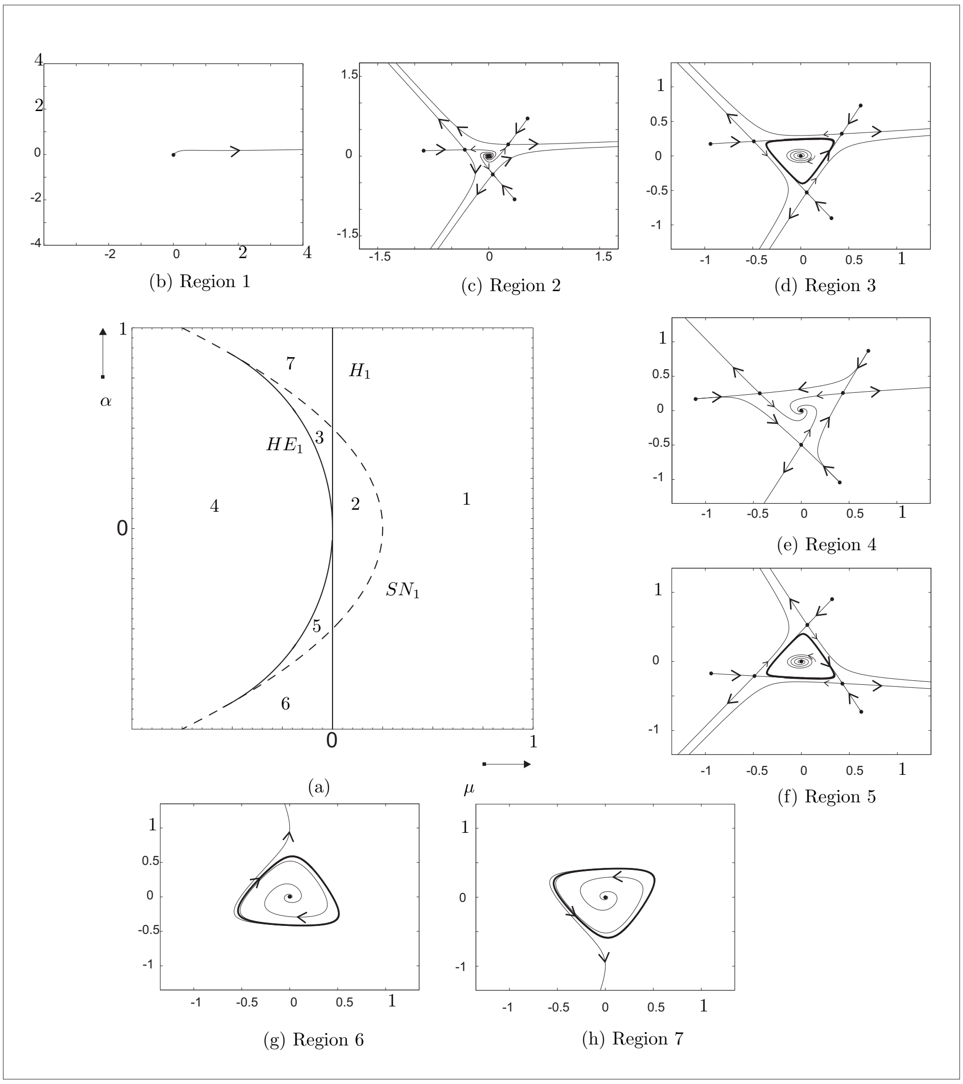

Fig. 4. (a) Two-dimensional bifurcation diagram of the 'principal part' for the k : 3 resonance (7) for $\theta_0 < \frac{\pi}{3}$; (b)-(h) Phase portraits for the indicated regions.

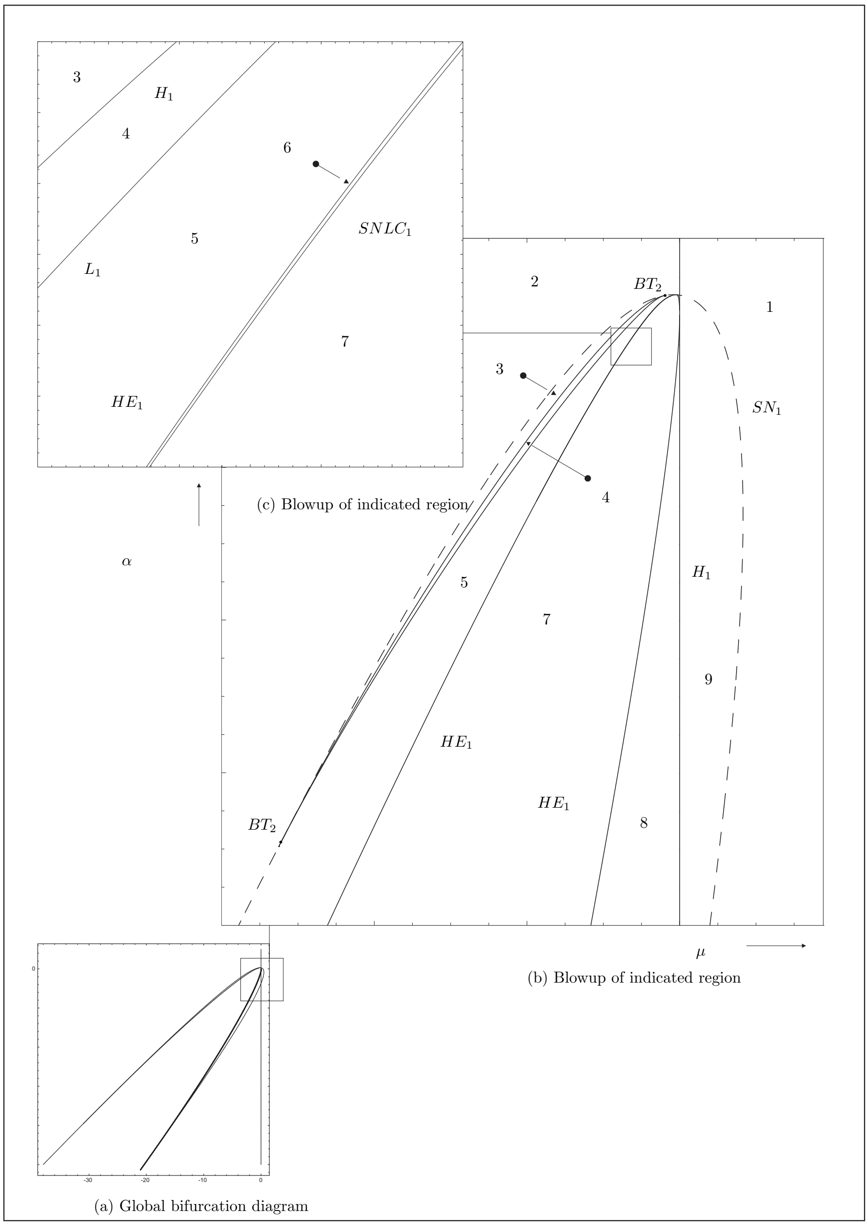

Fig. 5. (a) Two-dimensional bifurcation diagram of the ‘principal part’ for the $k : 3$ resonance (7) for $\theta_0 > \frac{\pi}{3}$; (b)-(c) Blowups of the indicated rectangles. Phase portraits for the regions labelled $1, \ldots, 9$ are given in Fig. 6.

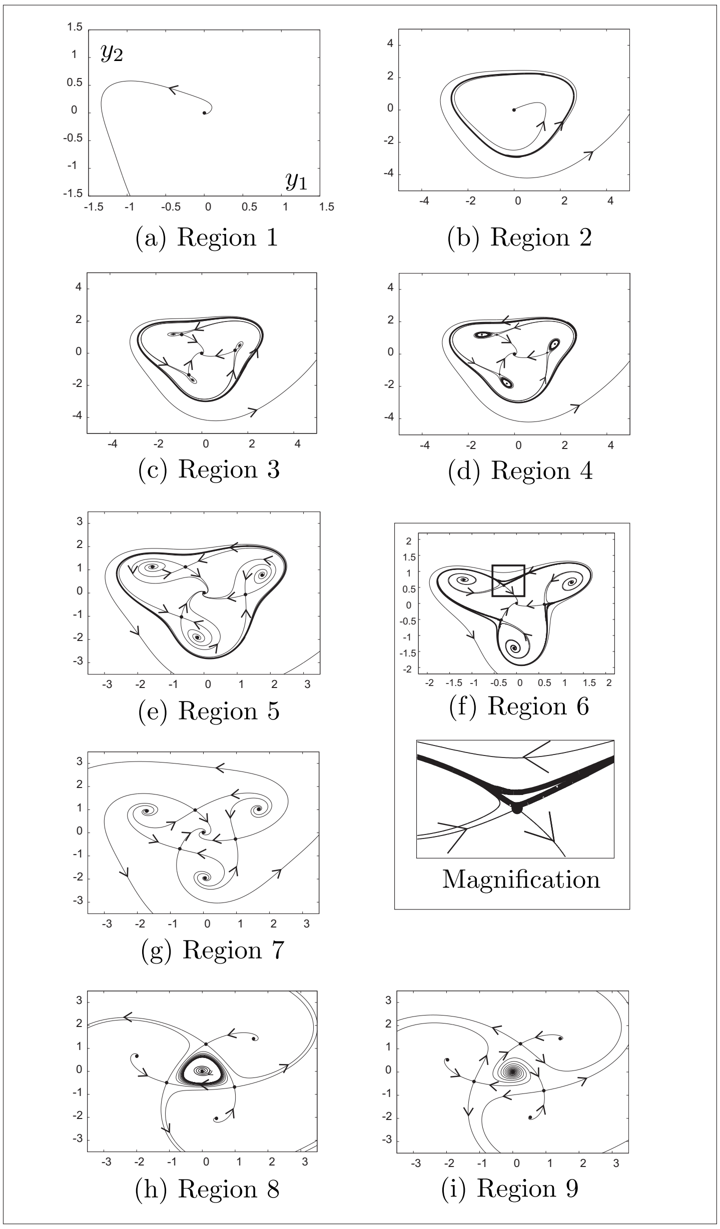

Fig. 6. (a)-(i) Phase portraits of the 'principal part' for the $k : 3$ resonance (7). The labels "Region 1 … 9" correspond to the regions in the bifurcation diagram in Fig. 5. Note that two limit cycles coexist in region 6, see the magnification.